https://doi.org/10.3311/PPch.14498

Periodica Polytechnica Chemical Engineering, 64(4), pp. 491–504, 2020

CO_2 Storage in Low Permeable Carbonate Reservoirs: Permeability and Interfacial Tension (IFT) Changes During CO_2 Injection in an Iranian Carbonate Reservoir

Mohammad Afkhami Karaei[1], Bizhan Honarvar[1*], Amin Azdarpour[1], Erfan Mohammadian[2,3**]

[1] Department of Chemical Engineering, Marvdasht Branch, Islamic Azad University, Marvdasht, Iran
[2] Department for Management of Science and Technology Development, Ton Duc Thang University, Ho Chi Minh City, Vietnam
[3] Faculty of Applied Sciences, Ton Duc Thang University, Ho Chi Minh City, Vietnam
* First corresponding author, e-mail: Honarvar2@gmail.com; **Second corresponding author, e-mail: erfan.mohammadian@tdtu.edu.vn

Received: 02 June 2019, Accepted: 26 August 2019, Published online: 10 October 2019

Abstract

The lack of fundamental experimental studies on low permeable carbonate reservoirs for CO_2 sequestration purposes is essential for further application of CO_2 sequestration as a highly-anticipated CO_2 mitigation method in deep saline aquifers, specifically those with low permeabilities. The core samples were taken from a carbonate reservoir in Iran and the brine composition was based on that of the same formation. The objective of this study is to investigate permeability alteration during CO_2 sequestration in the aquifers of a low permeable Iranian carbonate reservoir. Various parameters have been investigated. The effects of different parameters such as injection pressure, confining pressure, and temperature on permeability alteration of the cores was investigated. Moreover, the interfacial tension (IFT) of CO_2/brine was also determined at pressures and temperatures up to 7 MPa and 100 °C, respectively. The experimental results showed CO_2 solubility and rock dissolution to be the governing mechanism when CO_2 was injected into carbonate cores. The permeability measurements showed that permeability increases by increasing injection pressure and decreases by increasing confining pressure and temperature. The IFT measurement results showed that the IFT decreases significantly when there is an increase in pressure and temperature.

Keywords

low permeable, carbonate reservoirs, CO_2 sequestration, saline aquifer, Iranian reservoirs, IFT of CO_2/Brine

1 Introduction

Global warming is believed to be caused by an excessive consumption of fossil fuels. Over the past decade, CO_2 sequestration has gained considerable attention in the scientific community as a method to counteract the detrimental effects of global warming by safely storing large amounts of CO_2 in geological formations. Due to high occurrence and large storage capacity, aquifers are among the most suitable candidates for CO_2 sequestration. In this method, CO_2 is injected into deep saline aquifers, preferably more than 800 m deep, and stored in porous media via several mechanisms [1-4].

More than 50 % of the world's hydrocarbon reservoirs are classified as carbonate reservoirs. Approximately 70 % of middle-east hydrocarbon reserves can be found in carbonate reservoirs [5]. Although there have been some preliminary studies for application of CO_2 sequestration in the Middle East, there still exists a huge gap in the literature regarding the application of this method in (low permeable) carbonate reservoirs specifically in Iran.

The injection of the CO_2 into the saline aquifers and the CO_2 interactions with formation brine and formation rock is important from two perspectives. Injected CO_2 reacts with formation brine and creates an in-situ weak carbonic acid, which dissolves formation rock. Further, CO_2 can react with formation rock that contains reactive metal ions such as calcium and magnesium to form different precipitates, for example, calcium and magnesium carbonates [6, 7]. The precipitation of minerals is favored at high pH values versus low pH values [8]. The four mechanisms of CO_2 sequestration have been widely discussed in previous studies. [3, 8, 9].

Numerous studies [9-15] have examined CO_2 sequestration in saline aquifers with a focus on CO_2 solubility trapping mechanisms. Their findings showed that CO_2 solubility is greatly influenced by CO_2 pressure, temperature,

Cite this article as: Afkhami Karaei, M., Honarvar, B., Azdarpour, A., Mohammadian, E. "CO_2 Storage in Low Permeable Carbonate Reservoirs: Permeability and Interfacial Tension (IFT) Changes During CO_2 Injection in an Iranian Carbonate Reservoir", Periodica Polytechnica Chemical Engineering, 64(4), pp. 491–504, 2020. https://doi.org/10.3311/PPch.14498

and salinity. Some researchers reported findings of reduced permeability while others reported findings of increased permeability during CO_2 sequestration in saline aquifers. Information highlighting the density of CO_2 saturated brine, especially at reservoir conditions (high pressure and temperature), is crucial for determining the effectiveness of the CO_2 sequestration projects in saline aquifers. Literature survey on this matter revealed that, to date, limited work has been done specifically on carbonate reservoirs. The relationship between CO_2 solubility and its impact on the density of effluent brine and rock permeability is almost untouched in literature, hence the need for this study [14-19].

CO_2 injectivity is one of the major practical challenges during CO_2 injection into saline aquifers. In general, the parameters affecting well injectivity could be categorized as geomechanical effects, geochemical effects (precipitation and rock dissolution) and transport effects (fine mobilization) [20-24]. Rock and fluid interactions play vital role in changing the injectivity. Increasing the acidic strength of the formation brine via CO_2 dissolution in formation brine causes mineral dissolution and consequently increasing the permeability and injectivity. On the other hand, some of the minerals in solution could precipitate and block the pores, causing permeability impairment and reduced injectivity. In addition, salt precipitation may also occur during the injection of dry CO_2 into saline aquifers, causing reduced injectivity [25-29].

The study of Azin et al. [30] investigated CO_2 sequestration in carbonate aquifers with CO_2 pressure at 62 bar and temperature at 40 °C for 91 days. Their experiments showed that porosity and permeability of dolomite cores increased during the process. This was due to dolomite dissolution with CO_2, which then resulted in an increase of the concentration of Ca^{2+} and Mg^{2+} in effluent brine. Recently, Jeddizahed and Rostami [31] investigated the effects of injection rate and brine salinity during CO_2 injection into sandstone cores. Their results showed that salt precipitation occurs during the early stage of CO_2 injection. Increasing the brine salinity also increased the salt precipitation level which resulted in 21-66 % permeability reduction. Salt precipitation decreases with an increase in the injection rates, which caused 43-62 % permeability reduction. Although the aforementioned study is very helpful to get an insight about the mechanisms of the process, the temperature of the experiments was not really representative of that of the aquifers. Izgec et al. [32] investigated the effects of CO_2 injection on changes of porosity and permeability of the carbonate cores using CT-Scan method. They studied the effects of different brine salinities, CO_2 injection rate and temperature. Experimental results showed that both permeability increase and decrease can be obtained, and this behavior is very case sensitive. In general, the major mechanism for permeability changes could be related to CO_2 solubility and rock dissolution. In general, CO_2 solubility and acidic strength are deceased with increasing the salinity and temperature. Fewer ions in solution means less rock dissolution, thus decreasing the permeability.Kovacs et al. [33] conducted a very detailed study on injection CO_2 sequestration on low permeable carbonates in which a great number of variables and their contribution were considered. They used numerical reservoir simulation and carbonate cores from previous experiments carbonate to investigate the effectivity and mechanism of sequestration. They stated that rock dissolution is a controlling mechanism during CO_2 injection to the carbonate reservoir. The pH of brine is lowered by the dissolved CO_2 in brine, which can dissolve carbonate rocks and alter permeability and porosity of the rock. Although the study is very comprehensive, the permeabilities studied were 100 and 10 mD; one can argue that those values are not really reflecting the mechanisms in low permeable range. In a simulation study, Ghafoori et al. [34] examined CO_2 injection to carbonate and sandstone aquifers. They concluded that permeability changes do not influence equilibrium regions and the only effect that permeability has is on the injectivity. They further stated that the mineral trapping capacity of sandstone aquifers is higher than the carbonate aquifers during the CO_2 sequestration process. Although most of the aforementioned studies were carried out on carbonate cores, the range of permeabilities were from 4 to 100 mD.

Another important factor that affects the sequestration mechanisms of CO_2 in geological formation is fluid-rock and fluid-fluid interfacial tension [15, 18]. The most important interfacial property is the interfacial tension (IFT) between CO_2 and brine that saturates the caprock and pre-exist in the aquifers/reservoirs. IFT controls the flow of multiphase fluids in the porous media. Laplace equation (Eq. (1)) is the most commonly used capillary pressure equation via which the entry level pressure in a cylindrical pore throat is calculated:

$$P_c = \frac{2\delta_{w\text{-}CO2}\cos\theta}{R} \tag{1}$$

where $\delta_{w\text{-}CO2}$ is the interfacial tension between brine and CO_2, θ is the contact angle between CO_2/brine/surface,

and R is the radius of the largest pore throat of the caprock that is accessible to CO_2/brine interface. Alternatively, IFT could be calculated using the capillary storage capacity of CO_2 [35]. The maximum column height, H, of CO_2 that can be trapped in a given formation is given by Eq. (2):

$$H = \frac{2\delta_{w-CO2}\cos\theta}{\rho_b - \rho_{CO2}} \quad (2)$$

where g is the acceleration of gravity and ρ_b, ρ_{CO2} the densities of brine and CO_2, respectively. IFT between brine and CO_2 has been experimentally measured in some of the previous studies [35, 36]. It can be seen that IFT is controlled by the thermodynamic conditions of the experiments, such as pressure and temperature, as well as salinity and composition of brine.

Aggelopoulos et al. [36] investigated experimentally the effects of various salts and salinity of brines on changes of IFT between CO_2 and brine. They found that the increase in IFT of CO_2 and brine composed of two salts ($NaCl+CaCl_2$) is the sum of the two individual IFT increments due to each salt. In order to evaluate the efficiency of any CO_2 sequestration project in geological formations, the knowledge of range of the IFT and its changes based on thermodynamic/geological configuration of the repository of interest is essential [3, 36].

To the best of the authors' knowledge, no studies have been conducted on sequestration of CO_2 in very low permeable carbonate reservoirs, specifically in thermodynamic and geological conditions of Iranian reservoirs, where it can be observed that most of the literature focuses on simulation (often on field scale) [30, 31], or the experiments that are not really representative of geological conditions (pressure, temperature, salinity, pH) in low permeable carbonate aquifers [33].

The aim of the current study, therefore, is to investigate the feasibility of CO_2 sequestration in the aquifers of an Iranian carbonate oil reservoir. Since the major consequence of CO_2 dissolution in formation brine is permeability alteration via dissolution, this study also examines rock dissolution at a range of pressure, temperature and salinities. The effects of CO_2 injection pressure (1-7 MPa), formation rock confining pressure (5-15 MPa), temperature (27-100 °C), and salinity (119-294958 mg/kg) on rock permeability were investigated. In addition, the changes of IFT of CO_2/brine system under different pressure (1-7 MPa) and temperature (27-100 °C) conditions was experimentally investigated.

2 Experimental materials, setup and procedures

2.1 Reservoir characteristics

The cores used in this study were taken from a mature reservoir called Gadvan, located in southwest Iran. A detailed composition of the reservoir fluids is presented in Table 1. The reservoir under observation has an edge type aquifer with a thickness of 25 m and an encroachment angle of 360 degrees. The average permeability of aquifers is about 4.93 mD and its porosity is about 18 % and the aquifer temperature is 100 °C. The initial aquifer pressure is about 21.95 MPa while the current pressure is 11.67 MPa. The pressure of the aquifer has declined because of crude oil production from the reservoir. By crude oil production, reservoir pressure declines, thus, water from aquifer encroaches into the reservoir to compensate the reservoir oil pressure. This will result in pressure decline in the aquifer.

2.2 Fluids

Formation brine and sea water were used to represent the aqueous phase in this study. The total dissolved solids (TDS) of the formation brine was determined as 294,958 mg/kg (~30 wt. %) and sea water was determined as 35,079 mg/kg (3.5 wt. %). The components of formation brine and seawater are shown in Table 2. The formation brine was also collected from the aquifer in Gadvan

Table 1 Composition of reservoir fluid

Components	Mole fraction (%)
H_2S	0.00
N_2	0.36
CO_2	0.24
C_1	22.92
C_2	9.25
C_3	7.70
i-C_4	1.66
n-C_4	4.80
i-C_5	2.15
n-C_5	3.10
C_6	4.31
C_7	4.62
C_8	4.67
C_9	4.40
C_{10}	4.33
C_{11+}	25.49
C_{11+} Mole weight	
C_{11+} Specific Gravity	

reservoir, which is also the same reservoir from which core samples were taken. In addition to what is presented in Table 2, the physical properties of the formation brine were also determined and the results are shown in Table 3. The analytical grade of CO_2 used for all the experiments were of 99.9 % purity.

2.3 Core samples

The length and diameter of the core samples used in this study were 8.1 cm and 3.7 cm, respectively. Helium porosity and brine permeability methods were used to determine the average porosity and permeability of the core samples. Results showed the average porosity to be 16.27 % and permeability to be 4.81 mD. Table 4 summarizes the dimensions and properties of the reservoir cores used. X-ray powder diffraction (XRD) was conducted on the cores to identify the composition of the rock. Density of the rock samples were measured to be 2.87 g/cm^3.

Table 2 The composition of brines used in this study

Components	Formation brine (mg/kg)	Seawater (mg/kg)	Fresh water (mg/kg)
Na^+	107873	11100	14
K^+	2219	-	1
Ca^{2+}	4342	419	14
Mg^{2+}	536	1304	3
Sr^{2+}	338	-	<1
Ba^{2+}	1	-	1
Cl^-	177051	19350	15
HCO_3^-	257	146	37
SO_4^{2-}	2342	2690	33
Br^-	-	70	<1
TDS	294958	35079	119

Table 3 Physical properties of formation brine

Properties	Value
Salinity (mg/kg)	294,958
Water viscosity (cp)	0.586
Water compressibility coefficient (MPa^{-1})	3.10×10^{-4}
Density at reservoir condition (g/cc)	1.16
Formation volume factor (bbl/STB)	1.017
Specific gravity	1.139

Table 4 Characteristics of the reservoir core used in this study

Properties	Value
Length (cm)	8.10
Diameter (cm)	3.70
Bulk volume (cm^3)	87.09
Pore volume (cm^3)	14.17
Porosity (%)	16.27
Permeability (mD)	4.81

2.4 Apparatus

The schematic diagram of the coreflood setup used in this study is illustrated in Fig. 1. The main parts are a fluid accumulator, a core holder and a fluid collector. A syringe pump (ISCO 500D) with maximum working pressure of 25.85 MPa and maximum working flow rate of 200 cc/min was used to inject brine into the core samples. They were loaded into a high pressure stainless steel core holder that has a maximum operating pressure of 34.47 MPa. A back-pressure of 8.62 MPa was set at the back-pressure regulator. The differential pressures (DP) were then determined by using a pressure transducer. Following this, a liquid collector was deployed to collect the displaced brine and a gasometer was used to record the produced gas. The entire setup was placed inside an oven that has a temperature controller which allows for constant temperature experiments. The temperature, differential pressure and injection pressure were recorded with a data acquisition system and a computer.

For IFT measurement experiments, IFT400^{TM} with the maximum operating temperature of 205 °C and 21 MPa was used, as shown in Fig. 2. The pendant drop method was used to measure the IFT of the CO_2 and brine at reservoir conditions. A 50 cm^3 stainless steel chamber, with a glass window, was provided for taking the photographs. The IFT is then determined through the drop shape

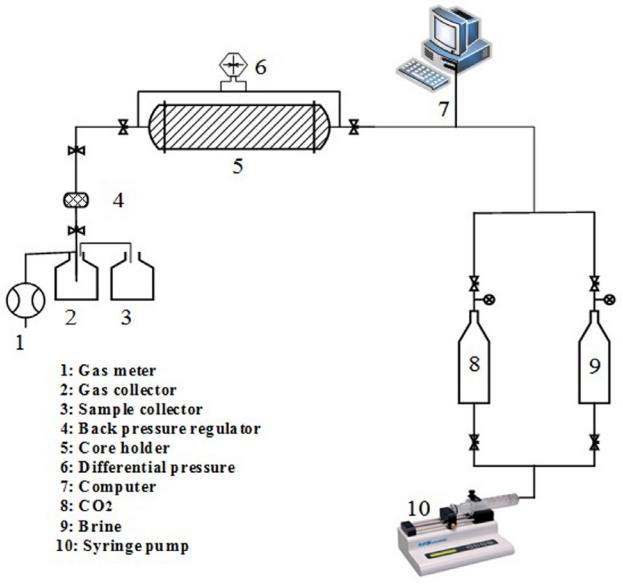

Fig. 1 Schematic diagram of coreflood system used in this study

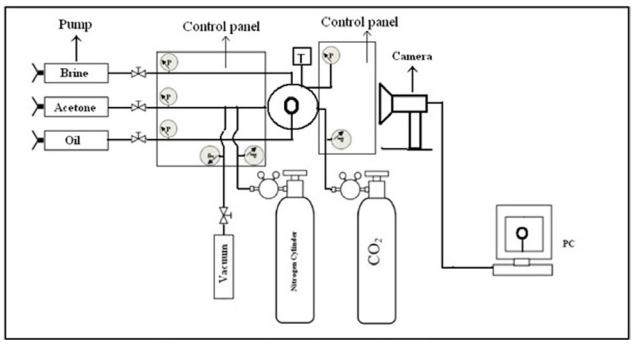

Fig. 2 Schematic diagram of IFT400

analysis technique. This is administered through an image processing code written by LabVIEW.

2.5 Experimental procedure

After the core samples were cleaned, dried and weighted, they were placed into the core holder. The initial air permeability is then measured at the ambient condition. The core holder was then vacuumed for 24 h. Afterwards, the formation brine was injected into the core and the brine permeability was measured accordingly. The permeability measurements were repeated three times and the uncertainties of the results were calculated to have an expanded relative uncertainty of 1.2 % with a coverage factor of 2.

The oven temperature was increased to 100 °C and maintained for about 12 h. Following that, the core samples were pressurized to 10 MPa by brine injection. Different pore volumes of the CO_2 with controlled constant injection rates (1-7 MPa) were injected into the core samples. After the injection, the core samples were depressurized and the oven temperature was reduced to ambient temperature. The injectivity reduction of the core samples was evaluated by injecting air into the core samples. Air permeability was then determined at the remaining water saturation (S_{wf}) level. These experiments were repeated by changing the different parameters such as different temperatures (27-100 °C), different injection pressures (1-7 MPa), and different confining pressures (5-15 MPa). The effect of the brine types on permeability was investigated by using three different brines which comprise formation brine, sea water and fresh water. After the experiments were completed, the effluent brine was collected and sent for further analysis. The pH value of each collected brine sample (including all the three types of brine used) was measured accordingly. Finally, the concentration of the calcium present in the effluent formation brine was measured by using inductively coupled plasma optical emission spectrometry (ICP-OES).

To measure the IFT, the entire system was initially checked for leakage with deionized water. It was then cleaned with acetone and deionized water before being flushed with nitrogen and evacuated [14]. At each pressure and after drop formation, a period of 600s (seconds) was needed to ensure thermodynamic equilibrium between the two phases [37, 38]. During this interval, IFT drops rapidly and then is stabilized by the same phenomenon that has been reported in a number of previous studies. [11, 15, 17, 18, 39, 40]. Before each measurement, a complete saturation of CO_2 and brine was achieved by injecting both phases to the cell and shaking them to reach an equilibrium condition of saturation. Then, the two equilibrium phases were separated at constant temperature and pressure. The density of each separate phase was accurately measured using an Anton PAAR digital high-pressure density meter. The equilibrium brine was extruded through the needle in the pendant drop apparatus, which was surrounded by equilibrium gas. Adequate time (10-12 h) was given to each solution to reach equilibrium condition and the IFTs were then determined accordingly. Drop sizes and shapes were also recorded from the visible segment of the sight cell. The uncertainties in IFT measurement were calculated to have an expanded relative uncertainty of 1.47 % with a coverage factor of 2. The expanded relative uncertainty of density was found to be 1.2 % with the coverage factor of 2.

3 Results and discussions

3.1 Effect of injection pressure on permeability

It is believed that CO_2 injection into brine saturated cores affect core permeability [30, 41-46]. Thus, different injection pressures (1-7 MPa) at the constant confining pressure of 10 MPa and temperature of 100 °C were applied. Core permeability was then determined. Each test was conducted using fresh water, formation brine and sea water. The results are presented in Fig. 3. The error bars showed 5 % of deviation from fresh water results.

The experimental results showed that the increasing injection pressure had a significant impact on core permeability. Clearly, core permeability increases with the increasing injection pressure. Moreover, it was observed that permeability was affected by salinity. At constant injection pressure, core permeability was higher in fresh water injection, followed by sea water injection and finally, formation brine injection. Taking the injection pressure of 1 MPa as an example, it was observed that permeability was 4.29 mD, 2.98 mD and 2.32 mD when fresh water,

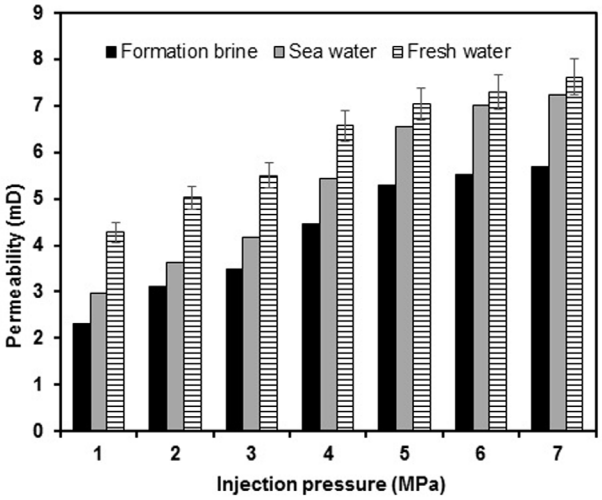

Fig. 3 Permeability changes with different injection pressures after 6 hours of injection at constant confining pressure of 10 MPa and 100 °C.

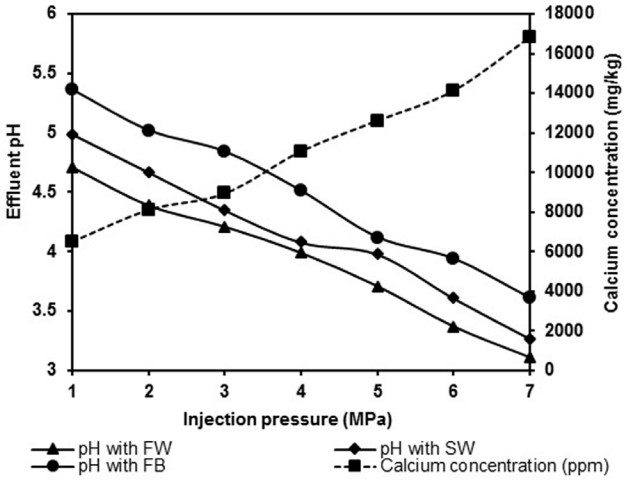

Fig. 4 Effluent pH and calcium concentration versus injection pressure at constant confining pressure of 10 MPa and 100 °C.

sea water and formation water were injected, respectively. In addition, at constant injection pressure of 7 MPa, permeability was determined to be 7.62 mD when fresh water was used, 7.24 mD when sea water was used and 5.69 mD when formation brine was used. Permeability reduction during CO_2 sequestration in aquifers is believed to be caused by salt precipitation, which results in reduced injectivity. It should be noted that in practical situations, it is very unlikely that fresh water is used for injection due to fiscal considerations, and injection of formation water is both technically and economically a more interesting option. It can be observed that using formation brine instead of freshwater in similar conditions of injection results in an average of 35 % reduction in permeability.

Permeability enhancement is caused by rock dissolution during CO_2 sequestration in aquifers. CO_2 solubility and reactivity increases with pressure. Previous studies have pointed out that a decrease in pH of the brine can be observed as the dissolution of CO_2 in brine is elevated by pressure, which creates a favorable condition for rock dissolution to occur [11, 47-50]. Therefore, in order to link the changes of permeability to the rock dissolution, the pH of effluents as well as calcium concentrations had to be determined after each coreflood experiment. Fig. 4 illustrates the pH of effluent brine and calcium concentration versus variable injection pressures at constant confining pressure of 10 MPa and 100 °C.

It can be seen from Fig. 4 that solution pH decreased with an increased injection pressure for all three types of brines used. However, this reduction was more severe when fresh water was used. This study suggests that CO_2 solubility is affected by several parameters, one of which is salinity. CO_2 solubility in fresh water was higher than in saline waters and this had resulted in a lower pH with fresh water [18, 48]. The latter can be observed in Fig. 4, where solution pH values was the highest in the formation brine, followed by sea water and finally fresh water.

As was discussed earlier, rock permeability increases with an increased pressure due to enhanced CO_2 solubility and increased rock dissolution. This inherently resulted in higher concentration of the Calcium cations in the effluent brine. As can be observed from Fig. 4, Calcium concentration increases with the increasing pressure regardless of type of the brine. This demonstrates that injection of CO_2 commences a chemical reaction between aqueous and solid phase. The mechanism of the reaction can be explained as follows. As CO_2 is injected, it dissolves in brine and produces carbonic acid. Then, carbonic acid dissociates into two components namely: hydrogen and bicarbonate ions, which results in drop of pH in solution (Eq. (3)). Finally, hydrogen ions attack the rock and dissolve it (Eq. (4)). Therefore, the amount of Mg^{2+} and Ca^{2+} ions increases in a solution. The mechanisms of dissolution of carbonates in aqueous solutions has been adequately discussed in previous studies [51, 52]:

$$CO_2(aq) + H_2O \leftrightarrow H^+(aq) + HCO_3^- \quad (3)$$

$$CaMg(CO_3)_2 + 2H^+(aq) \leftrightarrow Ca^{2+} + 2HCO_3^- \quad (4)$$

Moreover, the reduction in effluent pH is another indicator of increase in the concentration of carbonate ions in the brine or, in other words, higher solubility of CO_2 in

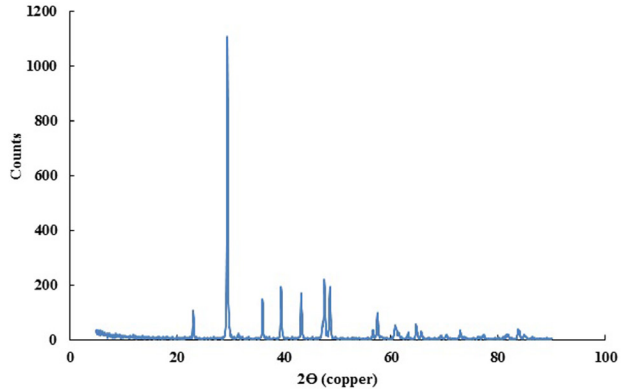

Fig. 5 XRD of the raw sample

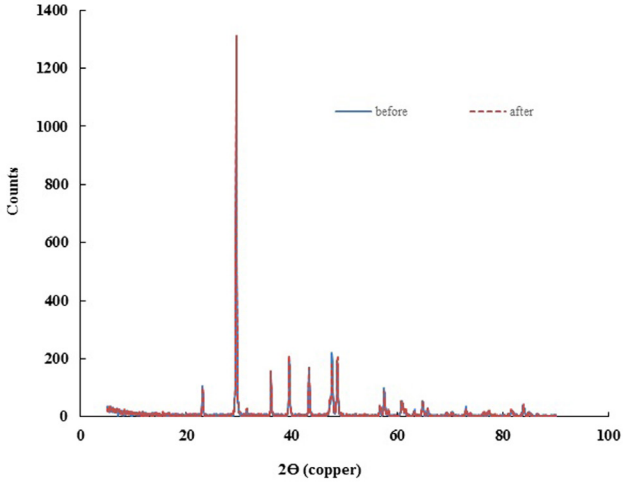

Fig. 6 XRD of the sample before and after the experiments

brine as pressure is increased. The decrease in solution pH with pressure has been reported in previous studies, both in carbonate and sandstone rocks [15, 50, 53].

Figs. 5 and 6 show the XRD image of the samples before and after the experiments, respectively. The peak at 29.5º illustrates the main composition of the clean rock sample (before any experiments) is dolomite $CaMg(CO_3)_2$ (2-5 wt. percent accuracy). It can be observed that the injection of CO_2 into the rock did not cause any change in the composition of the rock i.e. no CO_2 mineralization can be observed. The absence of CO_2 mineralization mechanism could be justified by pointing out that the reaction rate coefficient of CO_2 mineralization in carbonate rocks is considerably low, consequently the time scale required for this mechanism to naturally occur, without using any catalyst or any additional methods such as pH swing, is very long, in order of thousands of years [3, 50, 51]. Therefore, in the current study, the changes in mineralogy of the sample is assumed to be negligible.

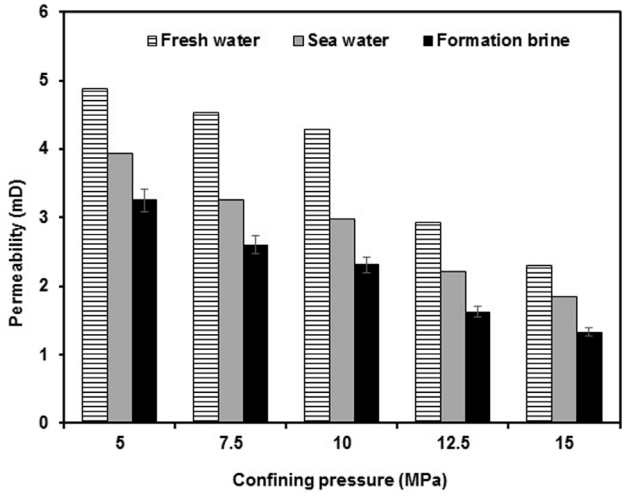

Fig. 7 Permeability changes with different confining pressures after 6 hours of injection at constant injection pressure of 1 MPa and 100 °C.

3.2 Effect of confining pressure on permeability

The effect of confining pressure on rock permeability was investigated under the confining pressure of 5-15 MPa at a constant injection pressure of 1 MPa and 100 °C. The brines tested were fresh water, sea water and formation brine. Fig. 7 displays the permeability changes with the variable confining pressures. The error bars show 5 % deviation from formation brine permeability. Regardless of the brine used, permeability reduced with the increased confining pressure. The lowest permeability was achieved under 15 MPa confining pressure and the highest permeability was accomplished under 5 MPa confining pressure. This trend is consistent in all the three tested brines (fresh water, sea water and formation brine). Nonetheless, brine type appears to affect rock permeability.

At constant operating condition (temperature and pressure), rock permeability was higher with fresh water, followed by sea water and finally, formation brine. At a constant confining pressure of 5 MPa, rock permeability was 4.87 mD with fresh water; 3.95 mD with sea water, and 3.26 mD with formation brine injection. These values reduced to 2.30, 1.85, and 1.33 mD, respectively, when under 15 MPa confining pressure. It can be observed from Fig. 7 that regardless of injection pressure, confining pressure significantly affects the reduction in permeability. As confining pressure increases, a reduction of 50 %, 53 %, and 60 % can be observed for fresh water, seawater, and formation brine, respectively. It can also be inferred from the results that the effects of confining pressure on reduction of permeability becomes more pronounced at higher salinities.

Confining pressure directly affects the effective stress-induced anisotropic tortuosity. Increasing the anisotropic tortuosity decreases the permeability. At constant injection pressure, increasing the confining pressure also increases the effective stress on the rock mass, which consequently reduces the pore space and caused rocks to shrink. This eventually increases the rock mass tortuosity for CO_2 movement, thereby resulting in reduced effective CO_2 permeability in the rock mass [47-51].

3.3 Effect of temperature on permeability of carbonate cores

Fig. 8 presents the permeability changes with respect to the different temperatures of 27, 38, 66, and 100 °C at the injection pressure of 1 MPa and a confining pressure of 10 MPa. Fig. 9 displays the effluent pH and calcium concentration versus temperature at constant injection pressure of 1 MPa and a confining pressure of 10 MPa. It seems clear that CO_2 solubility is the governing mechanism for rock dissolution during CO_2 sequestration in the aquifers. CO_2 solubility is reduced by increasing the temperature from 27 to 100 °C. This creates unfavorable conditions for rock dissolution. CO_2 solubility is also dependent on salinity where the higher the salinity, the lower the CO_2 solubility [54-56].

As shown in Fig. 8, permeability is reduced by increasing the temperature from 27 to 100 °C for all the three tested brines. The error bars in the Fig. 8 show 5% deviation from permeability in fresh water. As expected, permeability is higher when fresh water was used as opposed to sea water and formation brine. At a constant temperature of 27 °C, permeabilities of 7.73, 6.29, and 4.82 mD were achieved with fresh water, sea water and formation brine injection, respectively. The values decreased to 4.29, 2.98, and 2.32 mD, respectively, when the temperature was increased to 100 °C. The relationship between solution pH and CO_2 solubility is shown in Fig. 9 where increasing the salinity causes the CO_2 solubility to reduce significantly. This also reduces the acidic impact of CO_2. The pH measurement results also show that pH increases as temperature was increased; this can be explained by the reduced CO_2 solubility as temperature increased. At constant temperature, the highest pH was noted in the formation brine injection but the lowest pH was noted in fresh water injection. The outcome is due to the negative impact of salinity on CO_2 solubility. The impacts of composition and salinity of brines have been discussed in detail in the previous works on CO_2 solubility in brines [18, 57, 58].

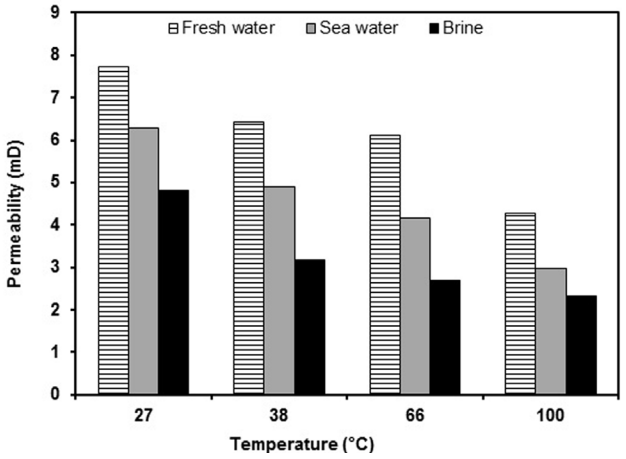

Fig. 8 Effect of temperature on permeability after 6 hours of injection at constant injection pressure of 1 MPa and confining pressure of 10 MPa.

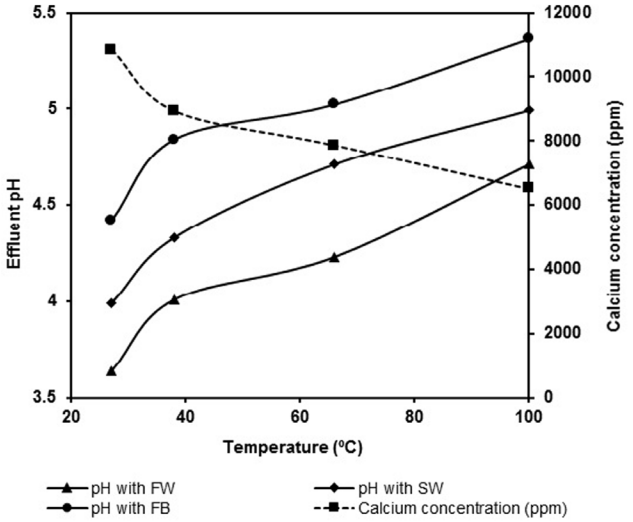

Fig. 9 Effluent pH and calcium concentration versus temperature at constant injection pressure of 1 MPa and confining pressure of 10 MPa

The amount of Calcium collected in the effluent core samples (see Fig. 9) also decreases as the temperature is increased. This also indicates that temperature adversely affects CO_2 solubility and rock dissolution.

3.4 Permeability changes with pressure, temperature and salinity

It is believed that rock dissolution during CO_2 injection into carbonate reservoirs is the major mechanism for permeability alteration. Rock dissolution is directly related to CO_2 solubility in water, in which the higher the CO_2 solubility, the higher the rock dissolution and the higher the permeability. Pressure, temperature, and salinity are the major parameters that affect CO_2 solubility and rock dissolution during CO_2 injection. By increasing the pressure, CO_2 solubility increases and then the solution become

more acidic. Consequently, rock dissolution increases, which results in a higher permeability with pressure. On the other hand, CO_2 solubility is reduced with temperature. This means, the acidic strength of the solution decreases with temperature, resulting in a less rock dissolution and less permeability with temperature. In addition, CO_2 solubility is reduced with salinity. Therefore, acidic strength and rock dissolution are reduced too, which results in lower rock dissolution and permeability with salinity [54, 56-58]. In brief, permeability is enhanced by increasing the pressure. On the other hand, decreasing the salinity and temperature increases the permeability.

3.5 Effects of temperature and pressure on IFT of CO_2-brine

Fig. 10 shows the effect of pressure (1-7 MPa) on the dynamic IFT, up to 2000s, hereafter stated in s, of formation brine with CO_2 at a constant temperature of 100 °C. Moreover, the changes in IFT, brine and CO_2 density with pressure and temperature are shown in Table 5. It can be observed that the IFT between brine and CO_2 decreases initially and after 600s reached a semi-plateau and after nearly 900s an equilibrium is achieved regardless of the pressure. The possible reason behind the decrease in IFT before 900s could be attributed to mutual dissolution of the two phases (CO_2/brine). The similar duration to achieve equilibrium (depending on the salinity of brine) has been reported in work of other researchers as well [35, 36].

The IFT data also shows that at any isotherm, increasing the pressure results in reducing the IFT between CO_2 and brine, hereafter referred to as IFT. The IFT decreased significantly by increasing the pressure from 1 to 7 MPa. The minimum and maximum IFTs of 20.15 and 37.56 mN/m were achieved under the injection pressure of 7 and 1 MPa, respectively. At low pressures, the decrease of IFT is noticeably sharper in comparison with those of higher pressures. The rate of IFT reduction is diminished at longer periods of time and reaches a plateau at around 900s at all the temperature series as can be seen in Figs. 10 and 11. The above mentioned behavior can be observed for all the isotherms. As an example, the changes of IFT versus time for various pressures at constant temperature of 100 °C is shown in Fig. 10.

On the other hand, increasing temperature had a different impact on the IFT of brine and CO_2 as shown in Fig. 11. Increasing the temperature negatively impacted the IFT, and resulted in an increase in IFT at constant injection pressure of 1 MPa. The minimum and maximum IFTs of

Table 5 Experimental values of IFT of formation brine and CO_2, Brine and CO_2 density at range of pressure and temperature

Temperature (°C)	Pressure (MPa)	Brine density (g.cm^{-3})	CO_2 density (g.cm^{-3})	IFT (mN/m)
27	1	1.211	0.018	25.96
27	2	1.180	0.039	24.18
27	3	1.130	0.063	23.92
27	4	1.140	0.092	22.17
27	5	1.152	0.128	20.43
27	6	1.156	0.183	19.50
27	7	1.161	0.710	18.80
38	1	1.101	0.017	30.96
38	2	1.109	0.037	29.16
38	3	1.118	0.059	28.12
38	4	1.131	0.084	25.91
38	5	1.136	0.115	24.12
38	6	1.142	0.153	21.15
38	7	1.145	0.207	19.33
66	1	1.067	0.016	35.83
66	2	1.071	0.033	29.95
66	3	1.089	0.052	27.88
66	4	1.084	0.073	25.18
66	5	1.109	0.096	24.02
66	6	1.116	0.124	21.42
66	7	1.121	0.141	19.9
100	1	1.126	0.014	37.56
100	2	1.153	0.031	35.70
100	3	1.186	0.045	33.97
100	4	1.190	0.062	29.63
100	5	1.193	0.082	26.93
100	6	1.195	0.912	23.97
100	7	1.198	0.12	20.15

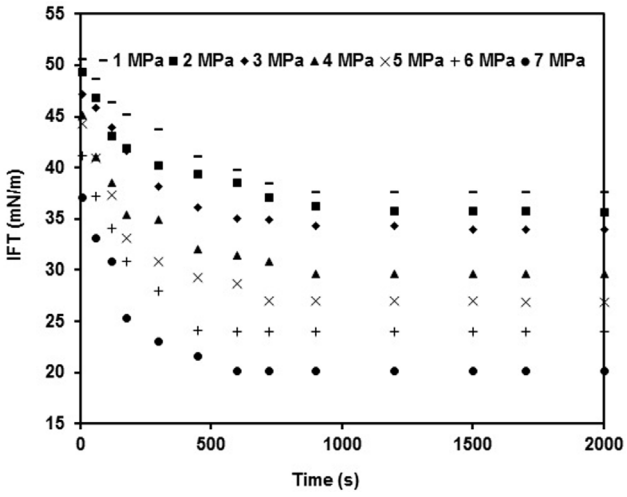

Fig. 10 Dynamic IFT of formation brine and CO_2 at constant temperature of 100 °C.

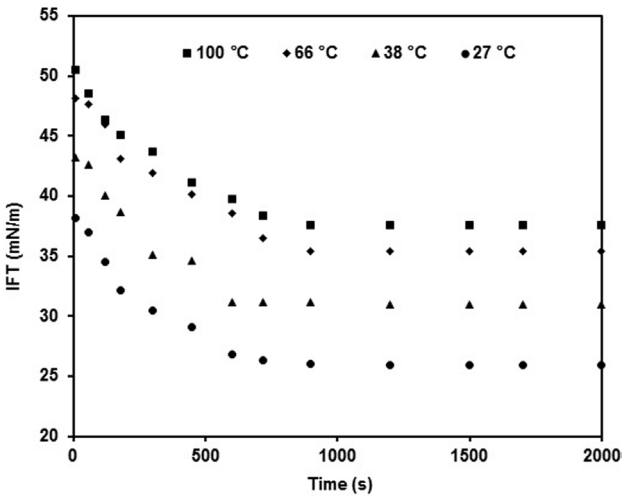

Fig. 11 Dynamic IFT of formation brine and CO_2 at constant pressure of 1 MPa.

25.96 mN/m and 37.56 mN/m were achieved under 27 and 100 °C, respectively.

It is also important to note that as temperature is increased, solubility of CO_2 in brine is reduced and therefore the IFT is adversely affected (increased). At 1MPa pressure, the CO_2 is at liquid state. Therefore, the solubility of CO_2 in brine is not very significant as compared to that of in supercritical state [3, 59, 60]. As a result, it can be seen that the changes in IFT values due to the reduction in dissolution is more dominant than the increase in IFT from temperature rise. Consequently, the IFT is reduced as temperature is increased at low pressures (below the critical point).

CO_2 solubility in brine is the governing mechanism when controlling the IFT of formation brine and CO_2. The higher the CO_2 solubility, the lower the IFT. CO_2 solubility in brine increases by increasing the pressure and decreases by increasing the temperature. As shown in Fig. 10, the minimum IFT of formation brine and CO_2 was achieved under the highest pressure of 7 MPa and the lowest IFT was achieved under the minimum pressure of 1 MPa. However, when it comes to the effect of temperature on IFT, the total entropy of two phase surface and entropy changes served as the primary governing mechanism while CO_2 solubility remains as the secondary mechanism. Increasing the temperature increases the mobility of the molecules and the kinetic energy. Thus, the total entropy of the two phase surface increases. This results in lower free energy (ΔG). Consequently, it lowers the IFT through temperature [61, 62].

Another observation noted from the drop analysis and IFT measurements is the shape and volume of the analyzed brine drops. Fig. 12 shows the typical images of the pendant drops under different pressure and temperature conditions. Fig. 12(a) presents brine drop under 1 MPa pressure (IFT is 37.56 mN/m), Fig. 12(b) presents brine drop under 7 MPa pressure (IFT is 20.15 mN/m), Fig. 12(c) presents brine drop under 27 °C temperature (IFT is 25.96 mN/m) and Fig. 12(d) presents brine drop under 66 °C temperature (IFT is 35.38 mN/m). As can be observed, the changes in the drop shape and volume are apparent. This is because of the CO_2 dissolution in brine decreases the IFT, hence resulting in bigger size drops and higher volumes.

The implication of the above results for practical sequestration projects is that the interaction between CO_2 and formation brine during CO_2 injection phase in aquifers, and the CO_2 displacement by invading brine during the CO_2 migration (imbibition) phase is controlled by pressure, temperature and composition of formation brine in the repository of interest [62-64]. Due to the effects that these primary variables have on the IFT between CO_2 and aquifer brine, which in turn affects capillary pressure and relative permeability, the effects of each of those parameters needs to be studied in detail for the repository of interest.

The current study can be enhanced in future by taking into account the effects of salinity and brine composition on changes of IFT and CO_2 solubility in carbonate reservoir. Moreover, longer time frames of the experiments on

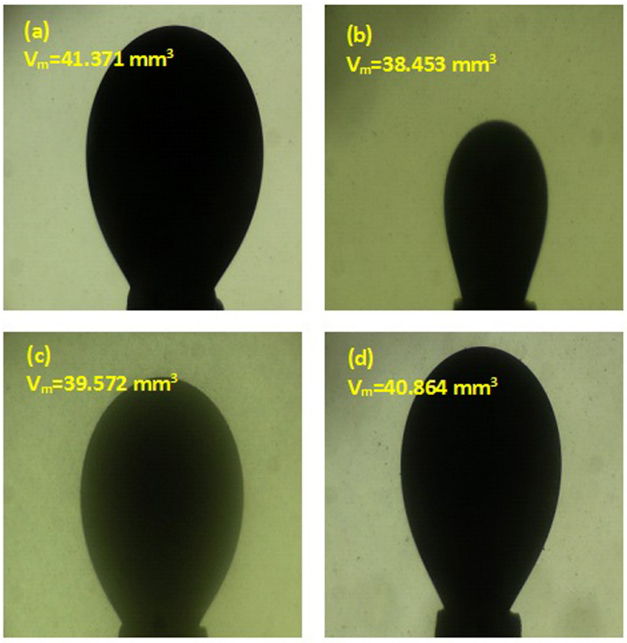

Fig. 12 Digital images of pendant drops of formation brine (a) under 1 MPa pressure; (b) under 7 MPa pressure; (c) under 27 ºC temperature; (d) under 66 °C temperature.

permeability alternation could be beneficial in observing the extent to which mineralization (mineral carbonation) occurs as CO_2 is injected to reservoirs/aquifers.

4 Conclusion

This study has investigated the effectiveness of CO_2 sequestration in the aquifers of an Iranian carbonate oil reservoir. Changes in rock permeability, viscosity and density of CO_2 saturated brines, and the IFT of CO_2 and brine were determined experimentally. The following conclusions could be drawn from the investigation conducted:

1. CO_2 solubility and consequently rock dissolution increased with pressure and decreased with temperature and salinity.
2. Permeability was increased with increasing CO_2 pressure regardless of the types of brine used. Under 1 MPa injection pressure, permeability was 4.29, 2.98, and 2.32 mD with fresh water, sea water, and formation brine, respectively. The values increased to 7.62, 7.24, and 5.69 mD, respectively, under 7 MPa pressure.
3. Permeability was reduced by increasing confining pressure. The lowest permeability was achieved under 15 MPa confining pressure and the highest permeability was accomplished under 5 MPa confining pressure.
4. Permeability was reduced by increasing the temperature from 27 to 100 °C for all the three tested brines. However, permeability was higher when fresh water was used as compared to sea water and formation brine.
5. Density of effluent brine decreased with increasing temperature. Brine density decreased from 1.1511 to 1.1261 g/cc by increasing the temperature from 27 to 100 °C.
6. The IFT decreased by increasing the pressure from 1 to 7 MPa. The minimum and maximum IFTs of 20.15 and 37.56 mN/m were achieved under the injection pressure of 7 and 1 MPa, respectively.
7. The IFT increased by increasing the temperature from 27 to 100 °C. The minimum and maximum IFTs of 25.96 mN/m and 37.56 mN/m were achieved under 27 and 100 °C, respectively.
8. CO_2 dissolution in brine decreases the IFT, hence resulting in bigger size drops and higher volumes.

Acknowledgment

The authors would like to gratefully acknowledge and appreciate the Department of Chemical Engineering, Faculty of Engineering, Marvdasht Islamic Azad University, Marvdasht, Iran, for the provision of the laboratory facilities necessary for completing this work.

References

[1] Szabó, Z., Hegyfalvi, C., Freiler-Nagy, Ágnes, Udvardi, B., Kónya, P., Király, C., Székely, E., Falus, G. "Geochemical reactions of Na-montmorillonite in dissolved scCO2 in relevance of modeling caprock behavior in CO2 geological storage", Periodica Polytechnica Chemical Engineering, 63(2), pp. 318–327, 2019. https://doi.org/10.3311/PPch.12850

[2] Nakhjiri, A. T., Heydarinasab, A. "CFD Analysis of CO2 Sequestration Applying Different Absorbents Inside the Microporous PVDF Hollow Fiber Membrane Contactor", Periodica Polytechnica Chemical Engineering, 2019. https://doi.org/10.3311/PPch.13172

[3] Kálmán, G., Réczey, K. "Possible ways of bio-refining and utilizing the residual lignocelluloses of corn growing and processing", Periodica Polytechnica Chemical Engineering, 51(2), pp. 29–36, 2007. https://doi.org/10.3311/pp.ch.2007-2.05

[4] Tsouris, C., Szymcek, P., Taboada-Serrano, P., McCallum, S. D., Brewer, P., Peltzer, E., Walz, P., Adams, E., Chow, E., Johnson, W. K., Summers, J. "Scaled-Up Ocean Injection of CO_2–Hydrate Composite Particles", Energy Fuels, 21(6), pp. 3300–3309, 2007. https://doi.org/10.1021/ef070197h

[5] Schlumberger. "Carbonate reservoirs: Meeting unique challenges to maximize recovery", Schlumberger, Paris, France, 2007.

[6] Ahmadi, M. A., Chen Z. "Analytical approach for leakage characterization in carbon sequestration in a bounded deep saline aquifer", Journal of Petroleum Science and Engineering, 169, pp. 772–784, 2018. https://doi.org/10.1016/j.petrol.2018.05.071

[7] Wei, B., Lu, L., Pu, W., Wu, R., Zhang, X., Li, Y., Jin, F. "Production dynamics of CO_2 cyclic injection and CO_2 sequestration in tight porous media of Lucaogou formation in Jimsar sag", Journal of Petroleum Science and Engineering, 157, pp. 1084–1094, 2017. https://doi.org/10.1016/j.petrol.2017.08.023

[8] Huijgen, W. J. J., Ruijg, G. R.,Comans, R. N. J., Witkamp, G. J. "Energy Consumption and Net CO_2 Sequestration of Aqueous Mineral Carbonation", Industrial and Engineering Chemistry Research, 45(26), pp. 9184–9194, 2006. https://doi.org/10.1021/ie060636k

[9] Chen, C., Chai, Z., Shen, W., Li, W. "Effects of Impurities on CO_2 Sequestration in Saline Aquifers: Perspective of Interfacial Tension and Wettability", Industrial and Engineering Chemistry Research, 57(1), pp. 371–379, 2018. https://doi.org/10.1021/acs.iecr.7b03873

[10] Li-ping, H., Ping-ping, S., Xin-wei, L., Qi-Chao, G., Cheng-sheng, W., Fangfang, L. "Study on CO_2 EOR and its geological sequestration potential in oil field around Yulin city", Journal of Petroleum Science and Engineering, 134, pp. 199–204, 2015. https://doi.org/10.1016/j.petrol.2015.06.002

[11] Riaz, A., Cinar, Y. "Carbon dioxide sequestration in saline formations: Part I—Review of the modeling of solubility trapping", Journal of Petroleum Science and Engineering, 124, pp. 367–380, 2014. https://doi.org/10.1016/j.petrol.2014.07.024

[12] Johnson, J., Scott, A. "Carbon Conundrum", Chemical & Engineering News, 91(7), pp. 12–15, 2013. Available at: https://cen.acs.org/articles/91/i7/Carbon-Conundrum.html [Accessed: 18 February 2013]

[13] Han, S. J., Wee, J. H. "Carbon Dioxide Fixation by Combined Method of Physical Absorption and Carbonation in NaOH-Dissolved Methanol", Energy Fuels, 31(2), pp. 1747–1755, 2017. https://doi.org/10.1021/acs.energyfuels.6b02709

[14] Bobicki, E.R., Liu, Q., Xu, Z., Zeng, H. "Carbon capture and storage using alkaline industrial wastes", Progress in Energy and Combustion Science, 38(2), pp. 302–320, 2012. https://doi.org/10.1016/j.pecs.2011.11.002

[15] Azdarpour, A., Asadullah, M., Mohammadian, E., Hamidi, H., Junin, R., Afkhami Karaei, M. "A review on carbon dioxide mineral carbonation through pH-swing process", Chemical Engineering Journal, 279, pp. 615–630, 2015. https://doi.org/10.1016/j.cej.2015.05.064

[16] Olajire, A. A. "A review of mineral carbonation technology in sequestration of CO2", Journal of Petroleum Science and Engineering, 109, pp. 364–392, 2013. https://doi.org/10.1016/j.petrol.2013.03.013

[17] Mohammadian, E., Hamidi, H., Asadullah, M. Azdarpour, A., Motamedi, S. Junin, R. "Measurement of CO_2 Solubility in NaCl Brine Solutions at Different Temperatures and Pressures Using the Potentiometric Titration Method", Journal of Chemical Engineering and Data, 60(7), pp. 2042–2049, 2015. https://doi.org/10.1021/je501172d

[18] Zhao, H., Dilmore, R., Allen, D. E., Hedges, S. W., Soong, Y., Lvov, S. N. "Measurement and Modeling of CO_2 Solubility in Natural and Synthetic Formation Brines for CO_2 Sequestration", Environmental Science and Technology, 49(3), pp. 1972–1980, 2015. https://doi.org/10.1021/es505550a

[19] Guo, H., Huang, Y., Chen, Y., Zhou, Q. "Quantitative Raman Spectroscopic Measurements of CO_2 Solubility in NaCl Solution from (273.15 to 473.15) K at p = (10.0, 20.0, 30.0, and 40.0) MPa", Journal of Chemical Engineering and Data, 61(1), pp. 466–474, 2016. https://doi.org/10.1021/acs.jced.5b00651

[20] Giorgis, T., Carpita, M., Battistelli, A. "2D Modeling of salt precipitation during the injection of dry CO_2 in a depleted gas reservoir", Energy Conversion and Management, 48(6), pp. 1816–1826, 2007. https://doi.org/10.1016/j.enconman.2007.01.012

[21] Alkan, H., Y. Cinar, Y., Ülker, E. B. "Impact of Capillary Pressure, Salinity and In situ Conditions on CO_2 Injection into Saline Aquifers", Transport in Porous Media, 84(3), pp. 799–819, 2010. https://doi.org/10.1007/s11242-010-9541-8

[22] Andre, L., Peysson, Y., Azaroual, M. "Well injectivity during CO_2 storage operations in deep saline aquifers - Part 2: Numerical simulations of drying, salt deposit mechanisms and role of capillary forces", International Journal of Greenhouse Gas Control, 22, pp. 301–312, 2014. https://doi.org/10.1016/j.ijggc.2013.10.030

[23] Yoo, S., Myojo, T., Matsuoka, T., Ueda, A. "Experimental Studies of Injectivity Reduction Due to Carbonate Mineralization", Procedia Earth and Planetary Science, 7, pp. 920–923, 2013. https://doi.org/10.1016/j.proeps.2013.03.166

[24] Kampman, N., Bickle, M., Wigley, M., Dubacq, B. "Fluid flow and CO_2-fluid-mineral interactions during CO_2-storage in sedimentary basins", Chemical Geology, 369, pp. 22–50, 2014. https://doi.org/10.1016/j.chemgeo.2013.11.012

[25] Ott, H., Roels, S. M., de Kloe, K. "Salt precipitation due to supercritical gas injection: I. Capillary-driven flow in unimodal sandstone", International Journal of Greenhouse Gas Control, 43, pp. 247–255, 2015. https://doi.org/10.1016/j.ijggc.2015.01.005

[26] Miri, R., Hellevang, H. "Salt precipitation during CO_2 storage—A review", International Journal of Greenhouse Gas Control, 51, pp. 136–147, 2016. https://doi.org/10.1016/j.ijggc.2016.05.015.

[27] Raza, A., Gholami, R., Rezaee, R., Bing, C. H., Nagarajan, R., Hamid, M. A. "Preliminary assessment of CO_2 injectivity in carbonate storage sites", Petroleum, 3(1), pp. 144–154, 2017. https://doi.org/10.1016/j.petlm.2016.11.008

[28] Adams Sokama-Neuyam, Y., Ginting, P. U. R., Timilsina, B., Ursin, J. R. "The impact of fines mobilization on CO_2 injectivity: An experimental study", International Journal of Greenhouse Gas Control, 65, pp. 195–202, 2017. https://doi.org/10.1016/j.ijggc.2017.08.019

[29] Cui, G., Wang, Y., Rui, Z., Chen, B., Ren, S., Zhang, L. "Assessing the combined influence of fluid-rock interactions on reservoir properties and injectivity during CO_2 storage in saline aquifers", Energy, 155, pp. 281–296, 2018. https://doi.org/10.1016/j.energy.2018.05.024

[30] Azin, R., Mehrabi, N., Osfouri, S., Asgari, M. "Experimental Study of CO_2–Saline Aquifer-Carbonate Rock Interaction during CO_2 Sequestration", Procedia Earth and Planetary Science, 15, pp. 413–420, 2015. https://doi.org/10.1016/j.proeps.2015.08.023

[31] Jeddizahed, J., Rostami, B. "Experimental investigation of injectivity alternation due to salt precipitation during CO_2 Sequestration in saline aquifers", Advances in Water Resources, 96, pp. 23–33, 2016. https://doi.org/10.1016/j.advwatres.2016.06.014

[32] Izgec, O., Demiral, B., Bertin, H., Akin, S. "CO_2 injection into saline carbonate aquifer formations I: laboratory investigation", Transport in Porous Media, 72(1), pp. 1–24, 2008. https://doi.org/10.1007/s11242-007-9132-5

[33] Kovacs, T., Poulussen, D.F., de Dios, J.C. "Strategies for injection of CO_2 into carbonate rocks at Hontomin", Global Carbon Capture and Storage Institute Ltd, Melbourne, Australia, 2015.

[34] Ghafoori, M., Tabatabaei-Nejad, S. A., Khodapanah, E. "Modeling rock-fluid interaction due to CO_2 injection into sandstone and carbonate aquifer considering sat precipitation and chemical reactions", Journal of Natural Gas Science and Engineering, 37, pp. 523–538, 2017.
https://doi.org/10.1016/j.jngse.2016.11.063

[35] Honarvar, B., Azdarpour, A., Karimi, M., Rahimi, A., Afkhami Karaei, M., Hamidi, H., Ing, J., Mohammadian, E. "Experimental Investigation of Interfacial Tension Measurement and Oil Recovery by Carbonated Water Injection: A Case Study Using Core Samples from an Iranian Carbonate Oil Reservoir", Energy Fuels, 31(3), pp. 2740–2748, 2017.
https://doi.org/10.1021/acs.energyfuels.6b03365

[36] Aggelopoulos, C. A., Robin, M., Vizika, O. "Interfacial tension between CO_2 and brine ($NaCl+CaCl_2$) at elevated pressures and temperatures: The additive effect of different salts", Advances in Water Resources, 34(4), pp. 505–511, 2011.
https://doi.org/10.1016/j.advwatres.2011.01.007

[37] Hosseini, T., Selomulya, C., Haque, N., Zhang, L. "Investigating the Effect of the Mg2+/Ca2+Molar Ratio on the Carbonate Speciation during the Mild Mineral Carbonation Process at Atmospheric Pressure", Energy Fuels, 29(11), pp. 7483–7496, 2015.
https://doi.org/10.1021/acs.energyfuels.5b01609

[38] Ampomah, W., Balch, R., Cather, M., Rose-Coss, D., Dai, Z., Heath, J., Dewers, T., Mozley, P. "Evaluation of CO_2 Storage Mechanisms in CO_2 Enhanced Oil Recovery Sites: Application to Morrow Sandstone Reservoir", Energy Fuels, 30(10), pp. 8545–8555, 2016.
https://doi.org/10.1021/acs.energyfuels.6b01888

[39] Zhang, Y., Lashgari, H. R., Sepehrnoori, K., Di, Y. "Effect of capillary pressure and salinity on CO_2 solubility in brine aquifers", International Journal of Greenhouse Gas Control, 57, pp. 26–33, 2017.
https://doi.org/10.1016/j.ijggc.2016.12.012

[40] Rathnaweera, T. D., Ranjith, P. G., Perera, M. S. A., Haque, A. "Influence of CO_2–Brine Co-injection on CO_2 Storage Capacity Enhancement in Deep Saline Aquifers: An Experimental Study on Hawkesbury Sandstone Formation", Energy Fuels, 30(5), pp. 4229–4243, 2016.
https://doi.org/10.1021/acs.energyfuels.6b00113

[41] Zendehboudi, S., Bahadori, A., Lohi, A., Elkamel, A., Chatzis, I. "Practical and Economic Aspects of the Ex-Situ Process: Implications for CO_2 Sequestration", Energy Fuels, 27(1), pp. 401–413, 2013.
https://doi.org/10.1021/ef301278c

[42] White, C. M., Smith, D. H., Jones, K. L., Goodman, A. L., Jikich, S. A., LaCount, R. B., DuBose, S. B., Ozdemir, E., Morsi, B. I., Schroeder, K. T. "Sequestration of Carbon Dioxide in Coal with Enhanced Coalbed Methane Recovery-A Review", Energy Fuels, 19(3), pp. 659–724, 2005.
https://doi.org/10.1021/ef040047w

[43] Zendehboudi, S., Khan, A., Carlisle, S., Leonenko, Y. "*Ex Situ* Dissolution of CO_2: A New Engineering Methodology Based on Mass-Transfer Perspective for Enhancement of CO_2 Sequestration", Energy Fuels, 25(7), pp. 3323–3333, 2011.
https://doi.org/10.1021/ef200199r

[44] Lee, Y., Kim, K., Sung, W., Yoo, I. "Analysis of the Leakage Possibility of Injected CO_2 in a Saline Aquifer", Energy Fuels, 24(5), pp. 3292–3298, 2010.
https://doi.org/10.1021/ef100073m

[45] Chen, C., Chai, Z., Shen, W., Li, W., Song, Y. "Wettability of Supercritical CO_2–Brine–Mineral: The Effects of Ion Type and Salinity", Energy Fuels, 31(7), pp. 7317–7324, 2017.
https://doi.org/10.1021/acs.energyfuels.7b00840

[46] Al-Yaseri, A., Zhang, Y., Ghasemiziarani, M., Sarmadivaleh, M., Lebedev, M., Roshan, H., Iglauer, S. "Permeability Evolution in Sandstone Due to CO_2 Injection", Energy Fuels, 31(11), pp. 12390–12398, 2017.
https://doi.org/10.1021/acs.energyfuels.7b01701

[47] Mohammadian, E., Motamedi, S., Shamshirband, S., Hashim, R., Junin, R.. Roy, C., Azdarpour, A. "Application of extreme learning machine for prediction of aqueous solubility of carbon dioxide", Environmental Earth Sciences, 75(215), pp. 1–11, 2016.
https://doi.org/10.1007/s12665-015-4798-4

[48] Azdarpour, A., Asadullah, M., Mohammadian, E., Junin, R., Hamidi, H., Manan, M., Daud, A. R. M. "Mineral carbonation of red gypsum via pH-swing process: Effect of CO_2 pressure on the efficiency and products characteristics", Chemical Engineering Journal, 264, pp. 425–436, 2015.
https://doi.org/10.1016/j.cej.2014.11.125

[49] Enick, R. M., Beckman, E. J., Shi, C., Xu, J., Chordia, L. "Remediation of Metal-Bearing Aqueous Waste Streams via Direct Carbonation", Energy Fuels, 15(2), pp. 256–262, 2001.
https://doi.org/10.1021/ef000245x

[50] Azdarpour, A., Asadullah, M., Mohammadian, E., Junin, R., Hamidi, H., Manan, M., Daud, A. R. M. "Mineral carbonation of red gypsum via pH-swing process: Effect of CO_2 pressure on the efficiency and products characteristics", Chemical Engineering Journal, 264, pp. 425–436, 2015.
https://doi.org/10.1016/j.cej.2014.11.125

[51] Wigand, M., Carey, J. W., Schütt, H., Spangenberg, E., Erzinger, J. "Geochemical effects of CO_2 sequestration in sandstones under-simulated in situ conditions of deep saline aquifers", Applied Geochemistry, 23(9), pp. 2735–2745, 2008.
https://doi.org/10.1016/j.apgeochem.2008.06.006

[52] Mohamed, I. M., He, J., Nasr-El-Din, H. A. "Permeability Change during CO2 Injection in Carbonate Aquifers: Experimental Study", In: Americas E&P Health, Safety, Security and Environmental Conference, Houston, Texas, USA, 2011, Article ID SPE-140979-MS.
https://doi.org/10.2118/140979-MS

[53] Hosseini, T., Selomulya, C., Haque, N., Zhang, L. "Indirect Carbonation of Victorian Brown Coal Fly Ash for CO_2 Sequestration: Multiple-Cycle Leaching-Carbonation and Magnesium Leaching Kinetic Modeling", Energy Fuels, 28(10), pp. 6481–6493, 2014.
https://doi.org/10.1021/ef5014314

[54] Hajiw, M., Corvisier, J., Ahmar, E. E., Coquelet, C. "Impact of impurities on CO_2 storage in saline aquifers: Modelling of gases solubility in water", International Journal of Greenhouse Gas Control, 68, pp. 247–255, 2018.
https://doi.org/10.1016/j.ijggc.2017.11.017

[55] Zhu, L., Liao, X., Chen, Z., Mu, L., Chen, X. "Analytical model for quick assessment of capillary storage capacity in saline aquifers", International Journal of Greenhouse Gas Control, 65, pp. 160–169, 2017.
https://doi.org/10.1016/j.ijggc.2017.09.004

[56] Steel, L., Liu, Q., Mackay, E., Maroto-Valer, M. M. "CO_2 solubility measurements in brine under reservoir conditions: A comparison of experimental and geochemical modeling methods", Greenhouse Gases: Science and Technology, 6(2), pp. 197–217, 2016.
https://doi.org/10.1002/ghg.1590

[57] De Silva, G. P. D., Ranjith, P. G., Perera, M. S. A. "Geochemical aspects of CO_2 sequestration in deep saline aquifers: A review", Fuel, 155, pp. 128–143, 2015.
https://doi.org/10.1016/j.fuel.2015.03.045

[58] Li, Y., Ranjith, P. G., Perera, M. S. A., Yu, Q. "Residual water formation during the CO_2 storage process in deep saline aquifers and factors influencing it: A review", Journal of CO2 Utilization, pp. 253–262, 2017.
https://doi.org/10.1016/j.jcou.2017.05.022

[59] Song, Y., Zhan, Y., Zhang, Y., Liu, S., Jian, W., Liu, Y., Wang, D. "Measurements of CO_2–H_2O–NaCl Solution Densities over a Wide Range of Temperatures, Pressures, and NaCl Concentrations", Journal of Chemical Engineering and Data, 58(12), pp. 3342–3350, 2013.
https://doi.org/10.1021/je400459y

[60] Yang, C., Gu, Y. "Accelerated Mass Transfer of CO_2 in Reservoir Brine Due to Density-Driven Natural Convection at High Pressures and Elevated Temperatures", Industrial and Engineering Chemistry Research, 45(8), pp. 2430–2436, 2006.
https://doi.org/10.1021/ie050497r

[61] Myers, D. "Surfaces, Interfaces and Colloids: Principles and Application", Jon Wiley & Sons Inc, New York, USA, 1999.
https://doi.org/10.1002/0471234990

[62] Moeini, F., Hemmati-Sarapardeh, A., Ghazanfari, M. H., Masihi, M., Ayatollahi, S. "Towards mechanistic understanding of heavy crude oil/brine interfacial tension: The roles of salinity, temperature and pressure", Fluid Phase Equilibria, 375, pp. 191–200, 2014.
https://doi.org/10.1016/j.fluid.2014.04.017

[63] Francke, H., Thorade, M. "Density and viscosity of brine: An overview from a process engineers perspective", Gheochemistry, 70(3), pp. 23–32, 2010.
https://doi.org/10.1016/j.chemer.2010.05.015

[64] Lu, C., Han, W. S., Lee, S. Y., McPherson, B. J., Lichtner, P. C. "Effects of density and mutual solubility of a CO_2-brine system on CO_2 storage in geological formations: “Warm” vs. “cold” formations", Advances in Water Resources, 32(12), pp. 1685–1702, 2009.
https://doi.org/10.1016/j.advwatres.2009.07.008